

Research Article

Unsteady Generalized Couette Flow in a Horizontal Channel with Sudden Application or Removal of a Porous Material

Michael O. Oni^{1*}, Aminat B. Yusuf², Taiwo S. Yusuf¹, Olaife H. Adebayo¹, Luqman A. Azeez³

¹Department of Mathematics, Ahmadu Bello University, Zaria, Nigeria

²Department of Information and Communication Technology, Usmanu Danfodiyo University, Sokoto, Nigeria

³Department of Primary Education, Federal College of Education, Zaria

Email: michaeloni29@yahoo.com

Received: 16 February 2022; Revised: 01 June 2022; Accepted: 06 June 2022

Abstract: The role of sudden application or removal of a porous material on generalized Couette flow in a horizontal channel is carried out. The governing momentum equation is obtained and solved with the necessary initial and boundary conditions. The well-known Laplace transform technique is employed to transform the PDEs into ODEs and then solved exactly in the Laplace domain. A numerical approximation based on the Riemann-sum is employed to transform the solutions obtained from the Laplace domain to the time domain. Based on the simulated results, it is found that the time taken to attain steady-state skin-friction and volumetric flow rate is strictly affected by the sudden application/withdrawal of porous medium. Also, despite the sudden application/withdrawal of porous medium, the velocities, skin-friction and volumetric flow-rates still attain steady state values.

Keywords: generalized Couette flow, porous material, unsteady

MSC: 76D05

1. Introduction

The scrutiny of flow formation in channels is a well-known problem in the literature due to its unending applications in the area of nuclear cooling, power generation, astrophysics, and solar winds. The generalized Couette flow on the other hand involves flow formation due to the combination of pressure gradient and impulsive motion of at least one of the plates. This phenomenon has significant application in drug delivery for cancer patients and design of micropumps. Couette [1] pioneered the flow formation due to the constant motion of one of the boundaries. Later, Mazumder [2] obtained an exact solution for Couette flow with oscillatory boundaries in a rotating system. Also, Akonur and Lueptor [3] examined the three dimensional velocity field for wavy Taylor-Couette flow while Jha and Apere [4-5] studied the unsteady MHD two-phase Couette flow of fluid-particle suspension and time-dependent MHD Couette flow of rotating fluid with Hall and ion-slip currents respectively. They found that the Hartmann number has retarding effect on fluid velocity.

The applications of flow formations in porous media cannot be overemphasized as they range from drying of porous solid, waste disposal, storage of grain coal, petroleum industry, aerodynamic stability and polymer technology.

Copyright ©2022 Michael O. Oni, et al.

DOI: <https://doi.org/10.37256/cm.3220221365>

This is an open-access article distributed under a CC BY license
(Creative Commons Attribution 4.0 International License)

<https://creativecommons.org/licenses/by/4.0/>

In the study of Couette flow formation in a composite channel filled with a porous material, Kuznetsov [6-7] carried out an analytical investigation of the fluid flow in the interface region between a porous medium and a clear fluid in channels partially filled with porous medium for Couette flow and no-slip flows respectively. Al-Nimr and Alkam [8] the transient behavior of non-Darcy fluid flow in parallel-plates channels partially filled with porous materials. Daskalakis [9] discussed the role of temperature dependent viscosity on Couette flow through a porous medium of a high Prandtl number. Jha et al. [10] studied the influence of transpiration on free convective Couette flow in a composite channel. In other works, Vafai and Kim [11] gave an exact solution for fluid mechanics of the interface region between a porous medium and a fluid layer while Jha and Odengle [12] and Jha and Apere offered a semi-analytical solution for MHD Couette flow in a composite channel and porous annulus respectively.

Inspired by the findings of Kumaran et al. [13] and Jha and Oni [14] where they numerically and analytically studied the transition of MHD boundary layer flow past a stretching sheet respectively. They found that the steady-state velocity and local skin friction varies with the magnetic field when there is a sudden application of magnetic field whereas unchanged for the sudden removal of the magnetic field. For exploration of crude oil and many other minerals, it is, therefore, significant to study the role of sudden application/withdrawal of porous material on generalized Couette flow formation in a horizontal channel. The novelty of this work is the establishment of analytical solutions to describe generalized Couette flow formation in a horizontal channel with sudden application or withdrawal of a porous material. These solutions deserve great attention as they have significant application in the area of crude-oil exploration and refinery.

2. Mathematical analysis

Consider the motion of incompressible, viscous, laminar fluid between two parallel plates filled with a porous material. The fluid exists in the region $0 \leq y' \leq h$ where the y' axis is the coordinate normal to the flow and h is the width of the channel. The fluid motion is fully developed hydrodynamically. The fluid flow inside the channel is set up by a combined pressure gradient in flow direction and motion of the lower plate with constant velocity u_0 which is located at $y' = 0$.

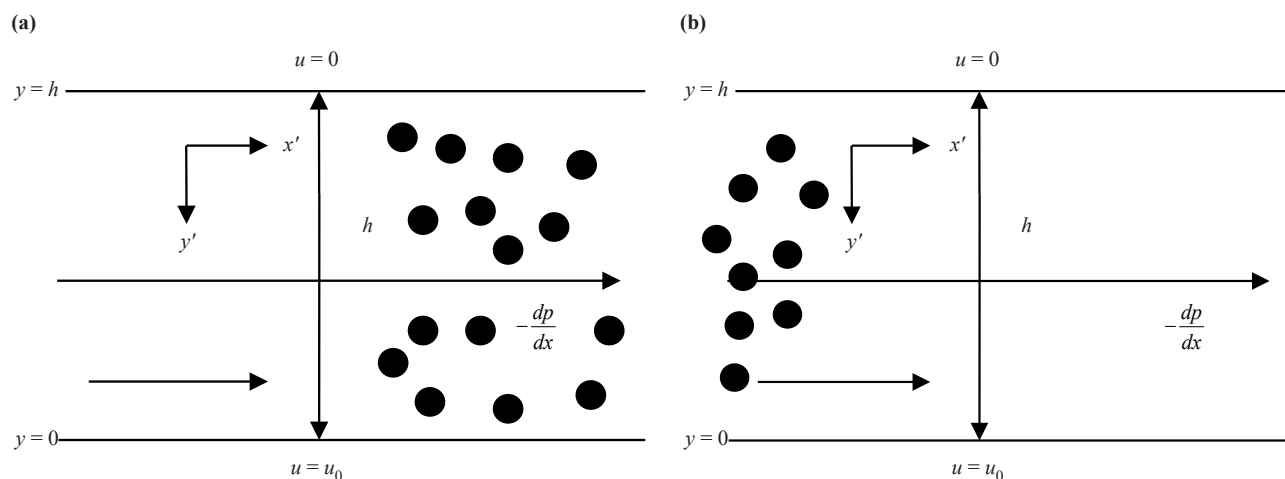


Figure 1. Schematic of the problem (a) Case I, (b) Case II

As the flow is fully developed and the plates are of infinite length, this means that all physical governing parameters are functions of y' and t' . Two cases are considered in this article, namely: case I (sudden application of a porous material) and case II sudden withdrawal of a porous material (see Figure 1).

2.1 Case I: Sudden application of a porous material

Following above assumption, and considering a steady, generalized Couette flow at initial state ($t = 0$); the mathematical model governing flow formation is given as:

$$\frac{d^2 u'_s}{dy'^2} = \frac{dps}{dx'} \quad (1)$$

With the boundary conditions:

$$u'_s = u_0; \text{ at } y' = 0$$

$$u'_s = 0; \text{ at } y' = h \quad (2)$$

By means of the ensuing non-dimensional quantities: $Y = y'/h$, $X = x'/h$, $u'_s = U_s/u_0$, where U_s is the non-dimensional steady-state velocity in the absence of porous material. Then equations (1) and (2) in dimensionless form become:

$$\frac{d^2 U_s}{dY^2} = \frac{dPs}{dX} \quad (3)$$

$$U_s = 1; \text{ at } Y = 0$$

$$U_s = 0; \text{ at } Y = 1 \quad (4)$$

The solution of (3) with boundary conditions (4) is:

$$U_s = \frac{dPs}{dX} \left[\frac{Y^2}{2} - \frac{Y}{2} \right] + (1 - Y) \quad (5)$$

The pressure gradient is obtained from [21],

$$\int_0^1 U_s(Y) dY = \int_0^1 dY \quad (6)$$

So that on solving for $\frac{dPs}{dX}$, the velocity U_s becomes:

$$U_s = 1 + 2Y - 3Y^2 \quad (7)$$

At $t' > 0$, a sudden porous material is applied throughout the fluid flow (Figure 1a). In this article, the equation for the unsteady generalized Couette flow filled with porous material is given in dimensionless form as:

$$\frac{\partial U_A}{\partial t} = \gamma \frac{\partial^2 U_A}{\partial Y^2} - \frac{H(t)U_A}{Da} - \frac{dP_A}{dX} \quad (8)$$

Where $Da = \frac{K}{h^2}$ is the Darcy number, K is the permeability and $H(t)$ is a unit step function; In this case:

$$H(t) = \begin{cases} 1 & \text{for } t > 0 \\ 0 & \text{for } t \leq 0 \end{cases} \quad (9)$$

Subject to the following initial and boundary conditions

$$t \leq 0, U_A = U_s, \quad 0 \leq Y \leq 1$$

$$t > 0 = \begin{cases} U_A = 1; & \text{at } Y = 0 \\ U_A = 0; & \text{at } Y = 1 \end{cases} \quad (10)$$

The solution of equation (8) subject to (10) can be obtained using the Laplace transform technique defined as follows:

$$\overline{U}_A(y, s) = \int_0^\infty U_A(y, t) e^{-st} dt, \text{ where } s > 0 \text{ for convergence.} \quad (11)$$

Taking the Laplace transform of equation (8), we obtain the following ordinary differential equation

$$\frac{d^2 \overline{U}_A}{dY^2} - \left(\frac{1}{Da} + S \right) \frac{\overline{U}_A}{\gamma} = \frac{1}{\gamma} \left[\frac{1}{s} \frac{dP_A}{dX} - (1 + 2Y - 3Y^2) \right] \quad (12)$$

The solution of equation (12) subject to boundary condition (10) is obtained as:

$$\begin{aligned} \overline{U}_A = & \frac{\sinh(\beta Y)}{\sinh(\beta)} \left[\frac{6Da^2}{(1+sDa)^2} - \left(\frac{1}{s} + \frac{Da}{s(1+sDa)} \frac{dP_A}{dX} - \frac{Da(1+sDa-6Da)}{(1+sDa)^2} \right) \cosh(\beta) + \frac{Da}{s(1+sDa)} \frac{dP_A}{dX} \right] \\ & + \cosh(\beta Y) \left[\frac{1}{s} + \frac{Da}{s(1+sDa)} \frac{dP_A}{dX} - \frac{Da(1+sDa-6Da)}{(1+sDa)^2} \right] \\ & - \frac{3DaY^2}{(1+sDa)} + \frac{2DaY}{(1+sDa)} - \frac{Da}{s(1+sDa)} \frac{dP_A}{dX} + \frac{Da(1+sDa-6Da)}{(1+sDa)^2} \end{aligned} \quad (13)$$

where $\beta = \sqrt{\frac{1+sDa}{\gamma Da}}$.

The skin-frictions at the walls $Y = 0$ and $Y = 1$ are respectively given as:

$$\tau_0 = \frac{d\overline{U}_A}{dY} \Big|_{Y=0} = \frac{\beta}{\sinh(\beta)} \left[\frac{6Da^2}{(1+sDa)^2} - \left(\frac{1}{s} + \frac{Da}{s(1+sDa)} \frac{dP_A}{dX} - \frac{Da(1+sDa-6Da)}{(1+sDa)^2} \right) \cosh(\beta) + \frac{Da}{s(1+sDa)} \frac{dP_A}{dX} \right] + \frac{2Da}{s(1+sDa)} \quad (14)$$

$$\tau_1 = \frac{d\overline{U}_A}{dY} \Big|_{Y=1} = \beta \cosh(\beta) \left[\frac{6Da^2}{(1+sDa)^2} - \left(\frac{1}{s} + \frac{Da}{s(1+sDa)} \frac{dP_A}{dX} - \frac{Da(1+sDa-6Da)}{(1+sDa)^2} \right) \cosh(\beta) + \frac{Da}{s(1+sDa)} \frac{dP_A}{dX} \right] + \beta \sinh(\beta) \left[\frac{1}{s} + \frac{Da}{s(1+sDa)} \frac{dP_A}{dX} - \frac{Da^2(Da-6(1+sDa))}{(1+sDa)^3} \right] - \frac{4Da}{(1+sDa)} \quad (15)$$

Also, the volumetric flow-rate in this current research is given in dimensionless form as:

$$Q_A = \int_0^1 \overline{U}_A dY = \frac{(\cosh(\beta)-1)}{\beta} \left[\frac{6Da^2}{(1+sDa)^2} - \left(\frac{1}{s} + \frac{Da}{s(1+sDa)} \frac{dP_A}{dX} - \frac{Da(1+sDa-6Da)}{(1+sDa)^2} \right) \cosh(\beta) + \frac{Da}{s(1+sDa)} \frac{dP_A}{dX} \right] + \frac{\sinh(\beta)}{\beta} \left[\frac{1}{s} + \frac{Da}{s(1+sDa)} \frac{dP_A}{dX} - \frac{Da^2(Da-6(1+sDa))}{(1+sDa)^3} \right] - \frac{Da}{s(1+sDa)} \frac{dP_A}{dX} + \frac{Da(1+sDa-6Da)}{(1+sDa)^2} \quad (16)$$

The above solutions govern the flow formation of generalized Couette flow in a horizontal channel with the sudden application of a porous material. These solutions are in the Laplace domain and need to be transformed to the time domain using the Riemann-sum approximation technique of Laplace inversion [18]. In this technique, any mathematical function in Laplace-domain can be inverted to the time-domain as follows [16-20]:

$$U_A(Y, t) = \frac{e^{\epsilon t}}{t} \left[\frac{1}{2} \overline{U}_A(Y, \epsilon) + \operatorname{Re} \sum_{n=1}^N \overline{U}_A(Y, \epsilon + \frac{i n \pi}{t}) (-1)^n \right] \quad 0 \leq Y \leq 1 \quad (17)$$

The Riemann-sum approximation for the Laplace inversion involves a single summation for the numerical process its accuracy depends on the value of ϵ and the truncation error dictated by N . According to Tzou [19], the value of ϵt that best satisfies the result is 4.7. In addition, it has been shown by [10, 12, 15] that the Riemann-sum approximation approach of Laplace inversion is a promising technique for obtaining high accuracy with an exact solution for a large value of n (in this work, the value of n with high accuracy is $n = 2000$).

2.2 Case II: Sudden withdrawal of porous material

Consider a generalized Couette steady flow formation in a horizontal channel filled with a porous material as depicted in Figure 1b. the lower plate at $y = 0$ is assumed to be moving with uniform velocity of U_0 while the plate $y = h$ is at rest. Flow formation is induced by the combined effect of pressure gradient as well as motion of the lower plate.

Based on the physics above, the principal momentum equation is achieved in dimensionless form as:

$$\frac{d^2 U_{ss}}{dY^2} - \frac{U_{ss}}{\gamma Da} = \frac{1}{\gamma} \frac{dP_{ss}}{dX} \quad (18)$$

$$U_{ss} = 1; \text{ at } Y = 0$$

$$U_{ss} = 0; \text{ at } Y = 1 \quad (19)$$

The solution to equation (18) with boundary condition (19) is given as:

$$U_{ss} = \left(1 + Da \frac{dP_{ss}}{dX}\right) \cosh\left(\frac{Y}{\sqrt{\gamma Da}}\right) + \frac{\left[\frac{dP_{ss}}{dX} Da \left(1 - \cosh\left(\frac{1}{\sqrt{\gamma Da}}\right)\right) - \cosh\left(\frac{1}{\sqrt{\gamma Da}}\right)\right] \sinh\left(\frac{Y}{\sqrt{\gamma Da}}\right)}{\sinh\left(\frac{1}{\sqrt{\gamma Da}}\right)} - Da \frac{dP_{ss}}{dX} \quad (20)$$

The pressure gradient is also obtained by the use of equation (8) as:

$$\frac{dP_{ss}}{dX} = \frac{\sinh\left(\frac{1}{\sqrt{\gamma Da}}\right) \left(1 - \sinh\left(\frac{1}{\sqrt{\gamma Da}}\right) \sqrt{\gamma Da}\right) + \left\{ \cosh\left(\frac{1}{\sqrt{\gamma Da}}\right) - 1 \right\} \sqrt{\gamma Da} \cosh\left(\frac{1}{\sqrt{\gamma Da}}\right)}{\sinh\left(\frac{1}{\sqrt{\gamma Da}}\right) Da \left[\sqrt{\gamma Da} \sinh\left(\frac{1}{\sqrt{\gamma Da}}\right) - 1 \right] - Da \sqrt{\gamma Da} \left(1 - \cosh\left(\frac{1}{\sqrt{\gamma Da}}\right)\right)^2} \quad (21)$$

Suddenly, the porous material is gradually removed following as follows:

$$H(t) = \begin{cases} 0 & \text{for } t > 0 \\ 1 & \text{for } t \leq 0 \end{cases} \quad (22)$$

So that

$$\frac{\partial U_W}{\partial t} = \frac{\partial^2 U_W}{\partial Y^2} - \frac{dP_W}{dX} \quad (23)$$

subjected to the initial and boundary conditions:

$$t \leq 0, U_W = U_{ss}, \quad 0 \leq Y \leq 1$$

$$t > 0, \begin{cases} U_W = 1; & \text{at } Y = 0 \\ U_W = 0; & \text{at } Y = 1 \end{cases} \quad (24)$$

Like previous case, by the use of Laplace transform technique, the solution to equation (23) subject to (24) is given

as:

$$\begin{aligned}
 U_W = C_5 \cosh(Y\sqrt{s}) + C_6 \sinh(Y\sqrt{s}) - \frac{1}{s} \frac{dP_W}{dX} - \frac{Da}{s} \frac{dP_{ss}}{dX} - \frac{\left(1 + Da \frac{dP_{ss}}{dX}\right) \gamma Da \cosh\left(\frac{Y}{\sqrt{\gamma Da}}\right)}{(1 - s\gamma Da)} \\
 - \frac{\left\{\frac{dP_{ss}}{dX} Da \left[1 - \cosh\left(\frac{1}{\sqrt{\gamma Da}}\right)\right] - \cosh\left(\frac{1}{\sqrt{\gamma Da}}\right)\right\} \gamma Da \sinh\left(\frac{Y}{\sqrt{\gamma Da}}\right)}{(1 - s\gamma Da) \sinh\left(\frac{1}{\sqrt{\gamma Da}}\right)} \quad (25)
 \end{aligned}$$

where

$$\begin{aligned}
 C_5 = \frac{1}{s} + \frac{1}{s} \frac{dP_W}{dX} + \frac{Da}{s} \frac{dP_{ss}}{dX} + \frac{\left(1 + Da \frac{dP_{ss}}{dX}\right) \gamma Da}{(1 - s\gamma Da)}, \\
 C_6 = \frac{1}{\sinh(\sqrt{s})} \left\{ \frac{1}{s} \frac{dP_W}{dX} + \frac{Da}{s} \frac{dP_{ss}}{dX} + \frac{\left(1 + Da \frac{dP_{ss}}{dX}\right) \gamma Da \cosh\left(\frac{1}{\sqrt{\gamma Da}}\right)}{(1 - s\gamma Da)} \right. \\
 \left. - C_5 \cosh(\sqrt{s}) + \frac{\left\{\frac{dP_{ss}}{dX} Da \left[1 - \cosh\left(\frac{1}{\sqrt{\gamma Da}}\right)\right] - \cosh\left(\frac{1}{\sqrt{\gamma Da}}\right)\right\} \gamma Da \cosh\left(\frac{Y}{\sqrt{\gamma Da}}\right)}{(1 - s\gamma Da) \sinh\left(\frac{1}{\sqrt{\gamma Da}}\right)} \right\}. \quad (26)
 \end{aligned}$$

Similarly, the skin-frictions at the walls $Y = 0$ and $Y = 1$ are respectively given as:

$$\tau_0 = \left. \frac{dU_W}{dY} \right|_{Y=0} = \sqrt{s} C_6 - \frac{\left\{\frac{dP_{ss}}{dX} Da \left[1 - \cosh\left(\frac{1}{\sqrt{\gamma Da}}\right)\right] - \cosh\left(\frac{1}{\sqrt{\gamma Da}}\right)\right\} \sqrt{\gamma Da}}{(1 - s\gamma Da) \sinh\left(\frac{1}{\sqrt{\gamma Da}}\right)} \quad (27)$$

$$\tau_1 = \left. \frac{d\overline{U}_W}{dY} \right|_{Y=1} = \sqrt{s} \left[C_5 \sinh(\sqrt{s}) + C_6 \cosh(\sqrt{s}) \right] - \frac{\left(1 + Da \frac{dP_{ss}}{dX} \right) \gamma Da \sinh\left(\frac{1}{\sqrt{\gamma Da}}\right)}{(1 - s\gamma Da)}$$

$$\frac{\left\{ \frac{dP_{ss}}{dX} Da \left[1 - \cosh\left(\frac{1}{\sqrt{\gamma Da}}\right) \right] - \cosh\left(\frac{1}{\sqrt{\gamma Da}}\right) \right\} \sqrt{\gamma Da} \cosh\left(\frac{1}{\sqrt{\gamma Da}}\right)}{(1 - s\gamma Da) \sinh\left(\frac{1}{\sqrt{\gamma Da}}\right)} \quad (28)$$

$$Q_W = \int_0^1 \overline{U}_W dY$$

$$= \frac{C_5}{\sqrt{s}} \left[\cosh(\sqrt{s}) - 1 \right] + \frac{C_6}{\sqrt{s}} \sinh(\sqrt{s}) - \frac{1}{s} \frac{dP_W}{dX} - \frac{Da}{s} \frac{dP_{ss}}{dX} - \frac{\left(1 + Da \frac{dP_{ss}}{dX} \right) \gamma Da \cosh\left(\frac{1}{\sqrt{\gamma Da}}\right)}{(1 - s\gamma Da)}$$

$$\frac{\left\{ \frac{dP_{ss}}{dX} Da \left[1 - \cosh\left(\frac{1}{\sqrt{\gamma Da}}\right) \right] - \cosh\left(\frac{1}{\sqrt{\gamma Da}}\right) \right\} \sqrt{\gamma Da} \left[\cosh\left(\frac{1}{\sqrt{\gamma Da}}\right) - 1 \right]}{(1 - s\gamma Da) \sinh\left(\frac{1}{\sqrt{\gamma Da}}\right)} \quad (29)$$

The above equations (25-29) describe flow formations of generalized Couette flow in a horizontal channel with the sudden withdrawal of porous material. These equations have significant application in the area of crude-oil exploration and refineries. Equations (25-29) are in the Laplace domain and must be transformed to the time domain following the procedure of (17).

3. Results and discussion

The role of sudden application/removal of a porous material on generalized Couette flow in a horizontal channel is carried out. The solutions obtained show that the sundry parameters explaining the physics of the current work are the Darcy number (Da) which is directly proportional to the permeability of the porous material, time (t) and the ratio of viscosities (γ). For a clearer understanding of the impact of various sundry parameters entering flow formations, figures are depicted to ascertain these effects.

Table 1 justifies the accuracy of the Riemann-Sum Approximation (RSA) by comparing the velocity profile using PDEPE. Pdepe is an inbuilt matlab function used to solve parabolic partial differential equations. This numerical comparison gives an excellent agreement.

Table 1. Numerical comparison of RSA and PDEPE for fluid velocity for sudden application of porous material

Y	t	$Da = 0.1$		$Da = 1.0$	
		RSA	PDEPE	RSA	PDEPE
0.0	0.2	1.0000	1.0000	1.0000	1.0000
	0.5	1.0000	1.0000	1.0000	1.0000
	1.0	1.0000	1.0000	1.0000	1.0000
0.0	0.2	0.7850	0.7851	1.2023	1.2023
	0.5	0.7771	0.7771	1.1939	1.1940
	1.0	0.7771	0.7770	1.1936	1.1937
0.0	0.2	0.5739	0.5738	1.1373	1.1372
	0.5	0.5605	0.5605	1.1231	1.1231
	1.0	0.5605	0.5604	1.1226	1.1225
0.0	0.2	0.4180	0.4181	0.8434	0.8434
	0.5	0.4072	0.4072	0.8319	0.8317
	1.0	0.4072	0.4070	0.8315	0.8314
0.0	0.2	0.0000	0.0000	0.0000	0.0000
	0.5	0.0000	0.0000	0.0000	0.0000
	1.0	0.0000	0.0000	0.0000	0.0000

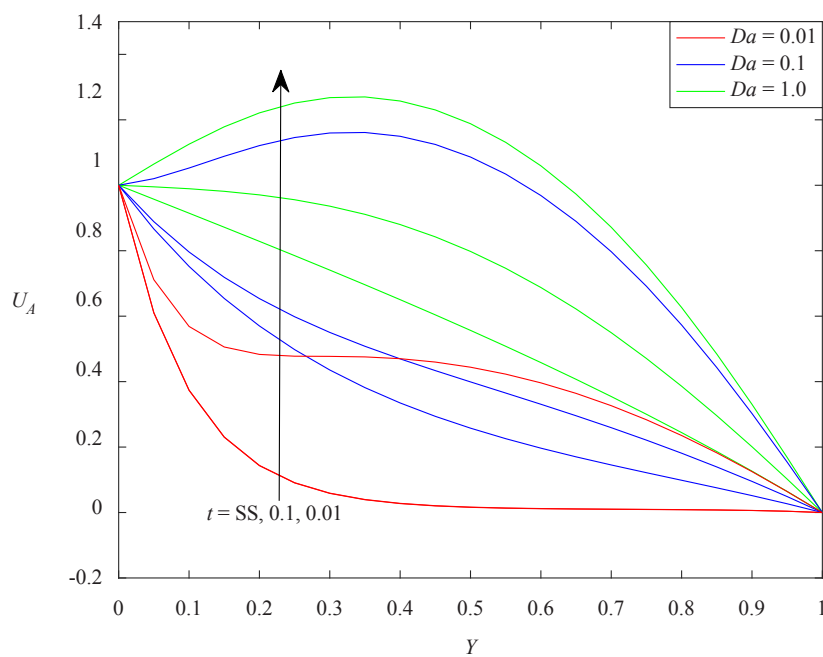


Figure 2. Velocity profile for different values of Da at different time

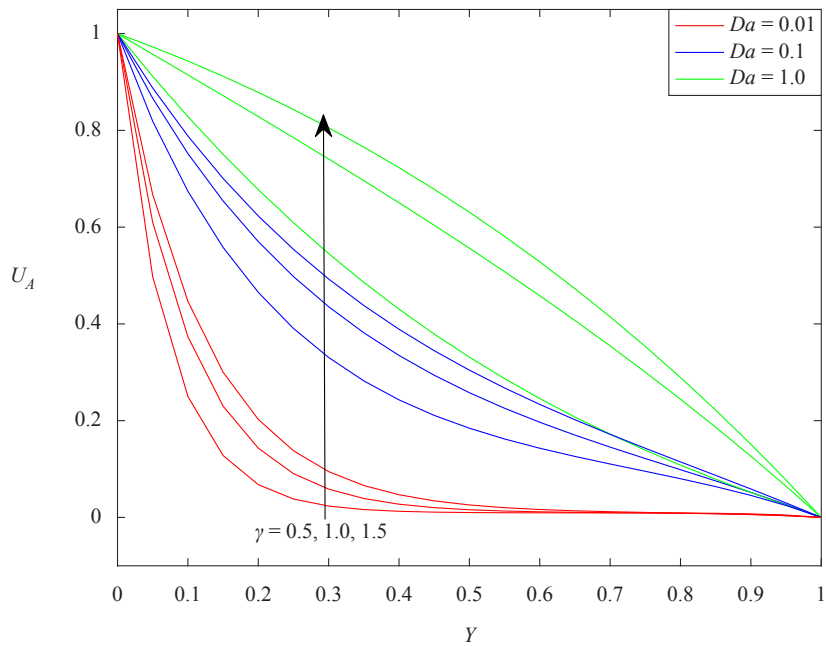


Figure 3. Velocity profile for different values of Da and γ at steady-state

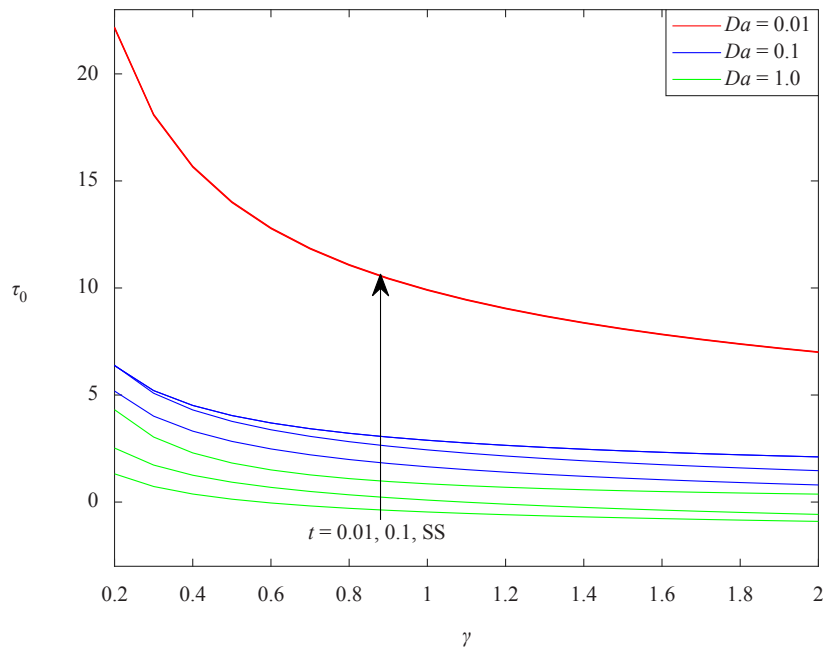


Figure 4. Skin-friction for different values of Da , γ and t at $Y = 0$

Figure 2 presents the impact of Darcy number which is inversely proportional to the permeability of the porous material on velocity profile for the case of sudden application of porous material at different times. It is revealed that the time taken for attainment of steady state velocity is strictly dependent on Da . In fact, a straight line is achieved for flow whose $Da = 1.0$ at a steady state. Figure 3 on the other hand describes the combined impact of Da and γ on the velocity

profile. It is obvious from this figure that fluid velocity increases with γ and Da . This could be attributed to the fact that an increase in Da increases the porosity and thereby increasing fluid velocity. Figure 4 depicts the skin-friction for different values of Da , γ time (t) at the wall $Y = 0$. It is noticed that the time required to attain steady state skin-friction is strictly dependent on Da but weakly dependent on γ .

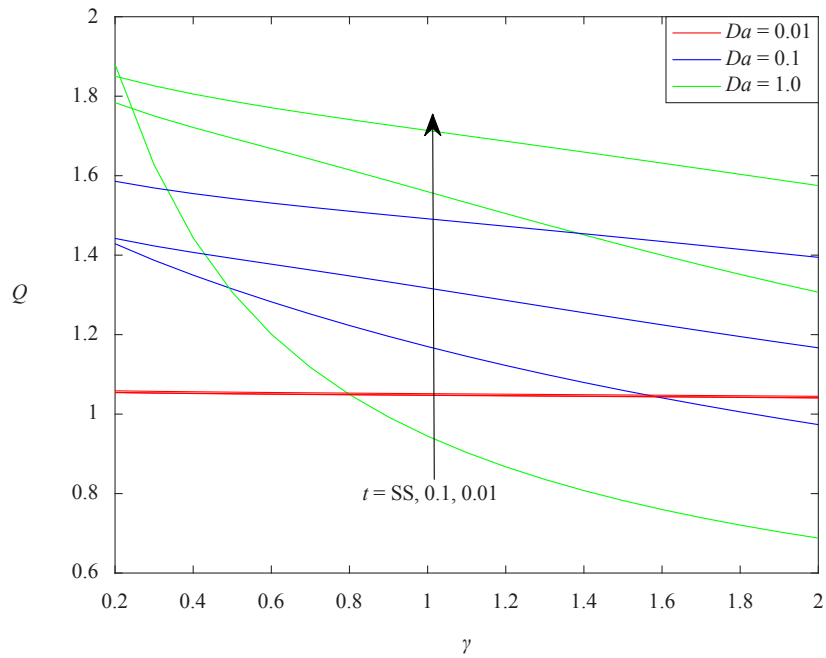


Figure 5. Volumetric flow-rate for different values of Da , γ and t

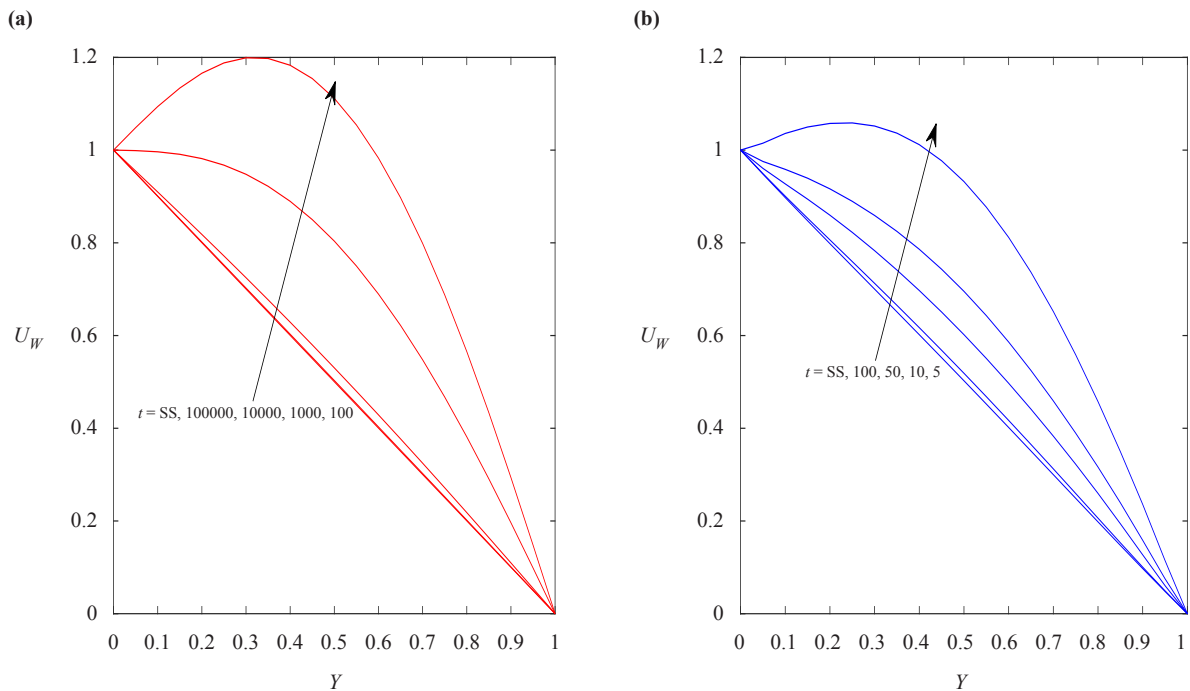


Figure 6. Velocity profile at different time for different values of Da (a) $Da = 0.1$, (a) $Da = 1.0$

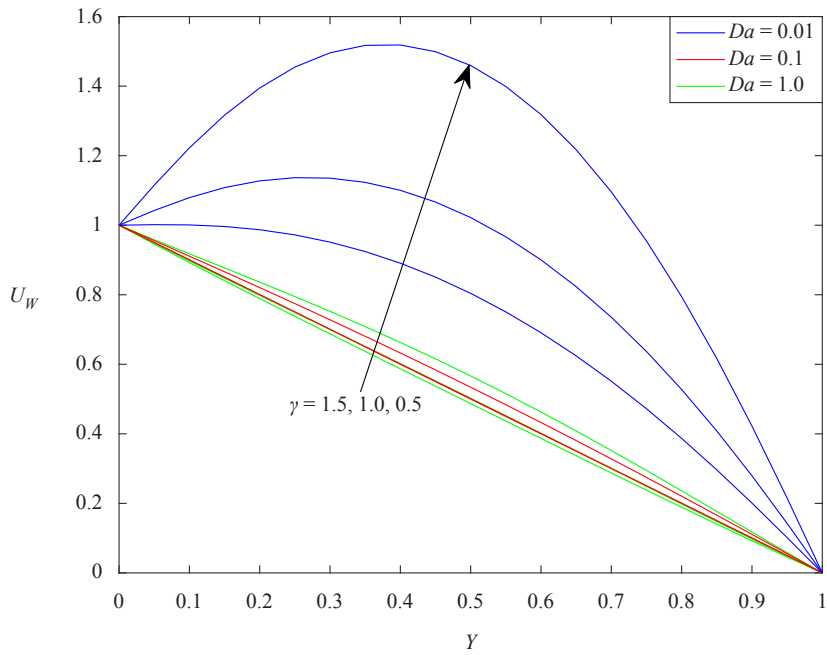


Figure 7. Velocity profile for different values of Da and γ

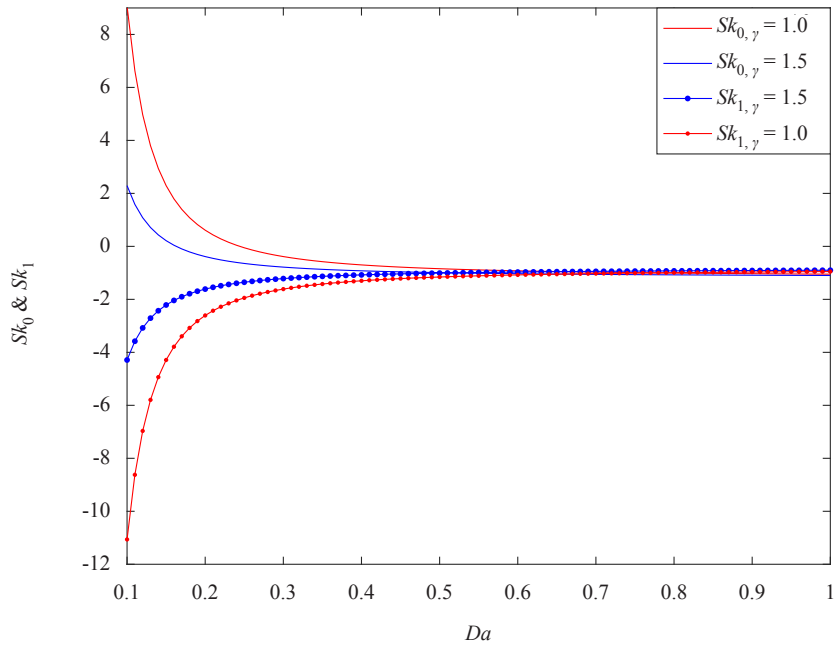


Figure 8. Skin-friction for different values of Da and γ

In fact, the time required to attain steady-state skin-friction is directly proportional to Da . Also, the maximum skin-friction is achieved for the least value of Da . This could be attributed to the fact that an increase in Da increases the permeability of the porous material, which in turn reduces the force at which the fluid hits the surface of the channel.

For a proper understanding of the impact of Da on volumetric flow-rate, Figure 5 presents the volumetric flow-

rate as a function of Da , γ and time. It is obvious from this figure that the volumetric flow-rate is directly proportional to Da and inversely proportional to time. This is true based on the definition of Da ; which increases with an increase in permeability between the porous material.

Figures 6a and 6b depict the velocity profiles for the case of sudden withdrawal of porous material for different values of time at $Da = 0.1$ and $Da = 1.0$ respectively. It is found from both figures that relative to the case of sudden application of a porous material, the time taken to achieve steady-state velocity is inversely proportional to Da . In fact, the time taken to achieve a steady-state solution for this case is extremely high relative to those of sudden application of a porous material. For a proper understanding of the role of γ on the velocity profile for this current case, Figure 7 presents the combined impact of viscosity ratio (γ) and Da on the velocity profile. It is found that velocity profiles vary inversely with γ . Figure 8 on the other hand shows the skin-friction at both walls for different values of Da and γ . The asymmetry nature of skin-friction at both walls is observed regardless of the value of Da or γ . Figure 9 presents the effect of γ and Da on the volumetric flow-rate in the channel. It is observed that flow-rate is not sensitive to γ at high values of Da .

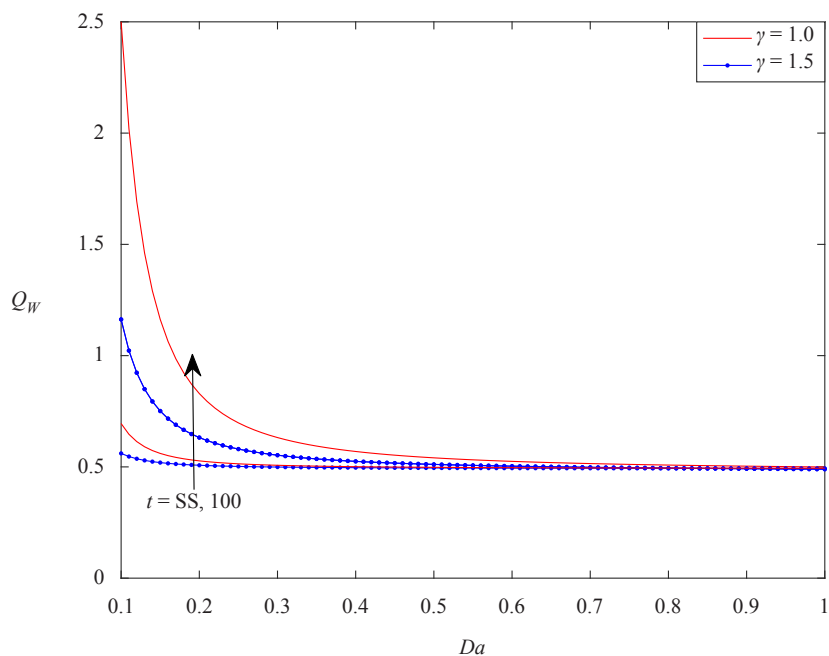


Figure 9. Volumetric flow-rate for different values of Da , γ and t

The overall results of velocity, skin-friction and volumetric flow-rate for sudden application of porous material show a reverse trend to those of sudden withdrawal of porous material.

4. Conclusions

Investigation of the role of sudden application/withdrawal of a porous material on forced convection generalized Couette flow in a horizontal channel is carried out in this article. The partial differential equations governing flow formations are gotten and solved analytically using the Laplace transform method. The major findings in this article are summarized as follows:

1. Fluid velocity for sudden application of porous material behave differently with sundry parameters from those of sudden withdrawal of porous material.

2. The time taken to attain steady-state solutions is extremely high in the case of sudden withdrawal of porous material.

3. The volumetric flow-rate and skin-friction and sudden application of porous material have a reverse trend with those of sudden withdrawal of porous material.

It is important to state that the results obtained from this article have significant applications in the exploration of crude-oil and hydrodynamics. Also, it is hoped that the obtained results will not only be useful in industrial and engineering fields but also serve as an improvement on previous studies. This work reduces to the work of Jha and Oni [15] when the porous material is replaced by a transversely applied magnetic field.

Conflict of interest

The author declares that there is no conflict of interest regarding the publication of this paper.

References

- [1] Couette MMAC. Etudes sur le frottement des liquids [Studies on the friction of liquid]. *Annales de chimie et de physique*. 1890; 21: 433-510.
- [2] Mazumder BS. An exact solution of oscillatory Couette flow in a rotating system. *ASME Journal of Applied Mechanics*. 1991; 58(4): 1104-1107.
- [3] Akonur A, Lueptor RM. Three dimensional velocity field for wavy Taylor-Couette flow. *Physics of Fluids*. 2003; 15: 947-960.
- [4] Jha BK, Apere CA. Unsteady MHD two-phase Couette flow of fluid-particle suspension. *Applied Mathematical Modelling*. 2013; 37(4): 1920-1931. Available from: <https://doi.org/10.1016/j.apm.2012.04.056>.
- [5] Jha BK, Apere CA. Time-dependent MHD Couette flow of rotating fluid with hall and ion-slip currents. *Applied Mathematics and Mechanics*. 2012; 33(4): 399-410. Available from: <https://doi.org/10.1007/s10483-012-1559-9>.
- [6] Kuznetsov AV. Analytical investigation of Couette flow in a composite channel partially filled with a porous medium and partially with clear fluid. *International Journal of Heat and Mass Transfer*. 1998; 41(16): 2556-2560.
- [7] Kuznetsov AV. Analytical investigation of the fluid flow in the interface region between a porous medium and a clear fluid in channels partially filled with porous medium. *Applied Scientific Research*. 1996; 56: 53-67.
- [8] Al-Nimr MA, Alkam MK. Unsteady non-Darcy fluid flow in parallel-plates channels partially filled with porous materials. *Heat and Mass Transfer*. 1998; 33: 315-318.
- [9] Daskalakis J. Couette flow through a porous medium of a high Prandtl number fluid with temperature dependent viscosity. *International Journal of Heat and Mass Transfer*. 1990; 14: 21-26.
- [10] Jha BK, Odengle JO, Kaurangini ML. Effect of transpiration on free convective Couette flow in a composite channel. *Journal of Porous Media*. 2011; 14(7): 627-635.
- [11] Vafai K, Kim SJ. Fluid mechanics of the interface region between a porous medium and a fluid layer-an exact solution. *International Journal of Heat and Fluid Flow*. 1990; 11(3): 254-256. Available from: [https://doi.org/10.1016/0142-727X\(90\)90045-D](https://doi.org/10.1016/0142-727X(90)90045-D).
- [12] Jha BK, Odengle JO. Unsteady MHD Couette flow in composite channel partially filled with porous material: A semi-analytical Approach. *Transport in Porous Media*. 2015; 107: 219-234.
- [13] Jha BK, Apere CA. Time-dependent MHD Couette flow in a porous annulus. *Communications in Nonlinear Science and Numerical Simulation*. 2013; 18(8): 1959-1969. Available from: <http://dx.doi.org/10.1016/j.cnsns.2013.01.008>.
- [14] Kumaran V, Kumar AV, Pop I. Transition of MHD boundary layer flow past a stretching sheet. *Communications in Nonlinear Science and Numerical Simulation*. 2010; 15(2): 300-311. Available from: <http://dx.doi.org/10.1016/j.cnsns.2009.03.027>.
- [15] Jha BK, Oni MO. Role of sudden application or withdrawal of magnetic field on mhd couette flow. *International Journal of Applied Mechanics and Engineering*. 2019; 24(4): 92-105. Available from: <https://doi.org/10.2478/ijame-2019-0051>.
- [16] Khadrawi AF, Al-Nimr MA. Unsteady natural convection fluid flow in a vertical microchannel under the effect of the Dual-phase-Lag heat conduction model. *International Journal of Thermophysics*. 2007; 28: 1387-1400.
- [17] Jha BK, Oni MO. Transient natural convection flow between vertical concentric cylinders heated/cooled

- asymmetrically. *Proceedings of the Institution of Mechanical Engineers, Part A: Journal of Power and Energy*. 2018; 232(7): 926-939. Available from: <https://doi.org/10.1177/0957650918758743>.
- [18] Jha BK, Oni MO. An analytical solution for temperature field around a cylindrical surface subjected to a time dependent heat flux: An alternative approach. *Alexandria Engineering Journal*. 2017; 57(2): 927-929. Available from: <https://doi.org/10.1016/j.aej.2017.01.003>.
- [19] Tzou DY. *Macro to microscale heat transfer: The lagging behaviour*. Washington: Taylor and Francis; 1997.
- [20] Oni MO, Jha BK. Theoretical analysis of transient natural convection flow in a vertical microchannel with electrokinetic effect. *Journal of Taibah University for Science*. 2019; 13(1): 1087-1099. Available from: <https://doi.org/10.1080/16583655.2019.1682830>.
- [21] Oni MO. Combined effect source, porosity and thermal radiation on mixed convection flow in a vertical annulus: An exact solution. *Engineering Science and Technology, an International Journal*. 2017; 20: 518-527.